

## **Facilitated photocatalytic H<sub>2</sub> production on Cu-coordinated mesoporous g-C<sub>3</sub>N<sub>4</sub> nanotubes**

Zhuizhui Su, Jianling Zhang,\* Zhonghao Tan, Jingyang Hu, Fengtao Zhang, Ran Duan, Lei Yao, Buxing Han, Yingzhe Zhao and Yisen Yang

Correspondence to: zhangjl@iccas.ac.cn (Jianling Zhang).

## 1. Materials and Methods

**Materials.** Urea (99% purity) and  $\text{CuCl}_2 \cdot 2\text{H}_2\text{O}$  (99% purity) were supplied by China National Medicines Co., Ltd. Melamine (99% purity),  $\text{H}_2\text{PtCl}_6 \cdot 6\text{H}_2\text{O}$  (99.9% purity) and triethanolamine (TEOA, A. R. grade) were purchased from Beijing InnoChem Science & Technology Co., Ltd. Ethanol (A. R. grade) and acetonitrile ( $\text{CH}_3\text{CN}$ , A. R. grade) were purchased from Beijing Chemical Works. Deionized water was provided by Beijing Analysis Instrument Factory. Nafion D-521 dispersion (5% w/w in water and 1-propanol,  $\geq 0.92$  meq/g exchange capacity) was purchased from Alfa Aesar China Co., Ltd. Ar and  $\text{N}_2$  (purity 99.9%) was supplied by Beijing Analysis Instrument Factory.

**Synthesis of P-CN.** In a typical experiment, urea (10 g) and melamine (1 g) were mixed evenly in a porcelain boat. Then the mixture was heated at 550 °C for 4 h with a heating rate 5 °C  $\text{min}^{-1}$  under a flow of Ar in a quartz tube furnace.

**Synthesis of P-CN(Cu).** Firstly, P-CN (200 mg) and  $\text{H}_2\text{O}$  (25 mL) were put into a 100 mL serum bottle and sonicated for 0.5 h. Then,  $\text{CuCl}_2 \cdot 2\text{H}_2\text{O}$  (12 mg) was added to the suspension and stirred at 40 °C for 9 h. The resulting product was washed three times with ethanol and dried in vacuum at 80 °C for 12 h. Finally, the dried powder was heated at 500 °C for 2 h with a heating rate 5 °C  $\text{min}^{-1}$  under a flow of Ar in a quartz tube furnace.

**Synthesis of B-CN.** Melamine (10 g) was put into a porcelain boat, and then heated at a muffle furnace at 500 °C for 4 h with a heating rate 5 °C  $\text{min}^{-1}$ .

**Material characterizations.** The morphologies were performed by SEM (HITACHI S-4800), TEM (JEM-1011) and HRTEM (JEM-2100F). The HAADF-STEM characterization was performed on a JEOL JEM-ARF200F TEM/STEM with a spherical aberration corrector. XRD patterns were detected on a Rigaku D/max-2500 diffractometer (Cu  $\text{K}\alpha$  radiation,  $\lambda = 1.5418 \text{ \AA}$ , 40 kV, 200 mA and 5°  $\text{min}^{-1}$ ). The elemental content of Cu in P-CN(Cu) was confirmed by ICP-AES. Solid-state  $^{13}\text{C}$  NMR spectra were collected using a Bruker Avance-400 spectrometer with a 4 mm zirconiarotor. XPS was recorded with a multipurpose X-ray photoemission spectroscopy (Thermo Scientific ESCALAB 250Xi). The UV-Vis DRS spectra were characterized by spectrophotometer (UV-2600, SHIMADZU). The transient state PL spectroscopy and steady-state PL spectra were obtained by a FLS980 fluorescence

spectrophotometer (the excitation wavelength of 405 nm) and a FluoroMax+ fluorescence spectrophotometer (the excitation wavelength of 370 nm), respectively. EPR spectra were collected on Bruker ELEXSYS II E500. X-ray absorption fine structure spectroscopy (XAFS) experiment was carried out at Beamline 1W1B at Beijing Synchrotron Radiation Facility. Data of XAFS were processed using Athena and Artemis programs of the IFEFFIT package based on FEFF 6. Data were processed with  $k^3$ -weighting and a Rbkg value of 1.0. Normalized XANES data were obtained directly from the Athena program of the IFEFFIT package. The porosity properties were gained from  $N_2$  adsorption-desorption analysis using a Micromeritics TriStarII system.

**Photocatalytic  $H_2$  production.** Typically, 5 mg of catalyst loaded with  $H_2PtCl_6$  (1 wt% Pt, co-catalysts) was dispersed in a mixture of  $CH_3CH/TEOA/H_2O$  (9 mL/1 mL/0.3 mL) in a flask. Then the system was purged with  $N_2$  for 1 h to remove air. The photocatalytic test was carried out at 25 °C and a 300 W Xe lamp equipped with a visible light cut-off filter ( $\lambda > 420$  nm) as the simulated light source. After irradiation for 3 h, the evolution gas was detected by gas chromatograph (GC, Agilent 8890) equipped with TCD detector using argon as the carrier gas. The  $H_2$  production rates were calculated after calibrating GC data. Photocatalytic stability of P-CN(Cu) was surveyed over three reaction cycles. After each cycle, the Xe lamp was turned off and the system was thoroughly flushed with  $N_2$  for 1 h before the next cycle started.

**Photoelectrochemical properties.** The photoelectrochemical measurement was performed on a three-electrode system (photocatalyst-coated indium-tin oxide as the working electrode, an Ag/AgCl with 3.5 M KCl as a reference electrode and 1 cm<sup>2</sup> Pt net as the counter electrode) at a CHI660E electrochemical workstation (Chenhua Instrument, Shanghai, China). The illumination source adopted in photocurrent ON/OFF cycles was a Xe lamp (300 W). A 0.5 M  $Na_2SO_4$  solution was used as electrolyte (pH = 6.8). In order to prepare the catalyst ink, the photocatalyst (5 mg) and 5 % Nafion 117 solution as conducting binder (15  $\mu$ L) were added into ethanol (250  $\mu$ L) and sonicated for 2 h. Then the catalyst ink was dropped on the surface of an indium-tin oxide (ITO) plate (1 cm<sup>2</sup>)/carbon paper (1 cm<sup>2</sup>) to prepare the working electrodes. LSV measurements, cyclic

voltammetry curves, Mott-Schottky measurements, transient photocurrents and EIS Nyquist plots were performed in 0.5 M Na<sub>2</sub>SO<sub>4</sub> solution.

**DFT calculations.** DFT-based first-principles calculations in this work were performed using Vienna ab initio simulation package (VASP) with projector-augmented wave (PAW) approach and the GGA-PBE exchange-correlation functional and the Heyd-Scuseria-Ernzerhof hybrid functional (HSE06) was implemented to examine and validate the electronic properties, the mixing parameter was 0.2. All calculations utilize a cutoff energy of 500 eV for the plane wave expansion. The k-points sampling is set as 2×2×1 for geometry optimizations. The convergence threshold for energy and atomic force is set as 1×10<sup>-5</sup> eV and 0.03 eV/Å, respectively. The DFT-D3 method of Grimme (D stands for dispersion) was used to account for van der Waals (vdW) interactions. We set the x and y directions parallel and the z direction perpendicular to the layer plane and adopted a supercell length of 20 Å in the z direction. The vacuum thickness is 20 Å.

The adsorption energy of H species ( $E_{\text{ads}}$ ) are taken as:

$$E_{\text{ads}}(\text{H}) = E_{\text{H+Slab}} - E_{\text{Slab}} - 1/2E_{\text{H}_2}$$

The free energy of adsorbed H ( $\Delta G_{\text{H}^*}$ ) of the above three systems are taken as:

$$\Delta G_{\text{H}^*} = \Delta E_{\text{H}^*} + \Delta E_{\text{ZPE}} - T\Delta S$$

where  $\Delta E_{\text{H}^*}$  is the adsorption energy of H species.  $\Delta E_{\text{ZPE}}$  and  $\Delta S$  are the difference of zero-point energy and entropy between H\* and the gas phase, respectively. T is the system temperature (298.15 K).

## 2. Results and Discussion

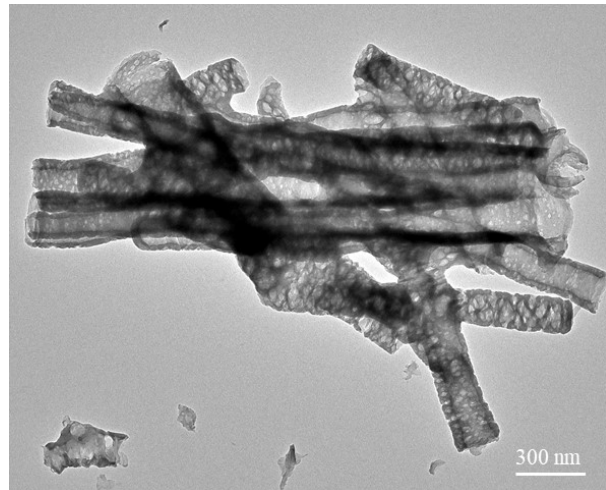


**Fig. S1.** TEM image of P-CN.

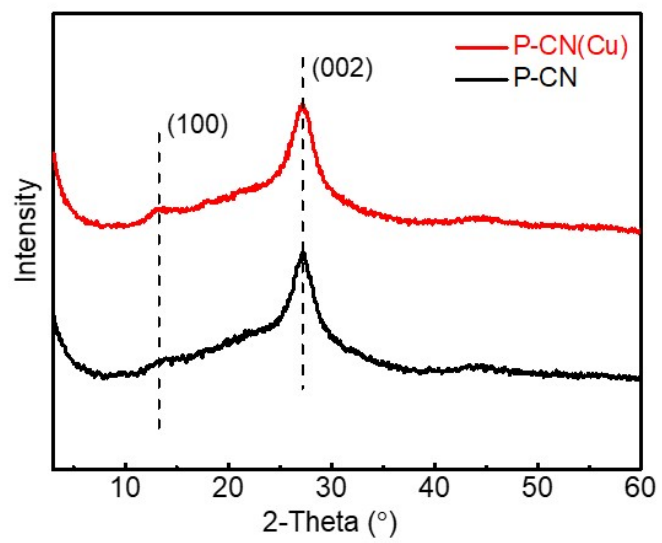


**Fig. S2.** XRD patterns of P-CN(Cu) and P-CN.

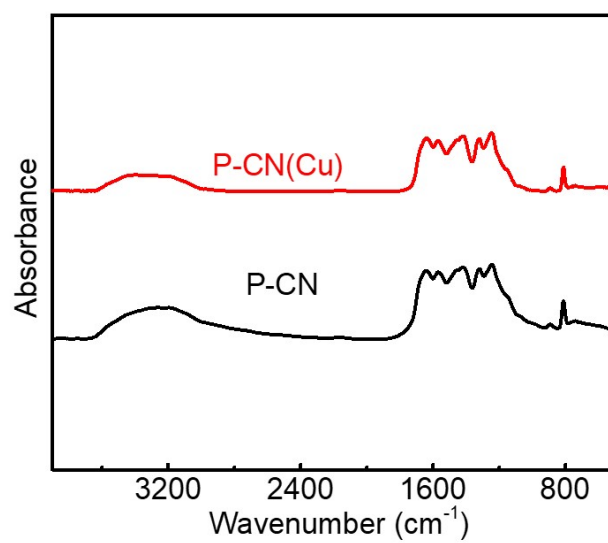


**Fig. S3.** FT-IR spectra of P-CN(Cu) and P-CN.

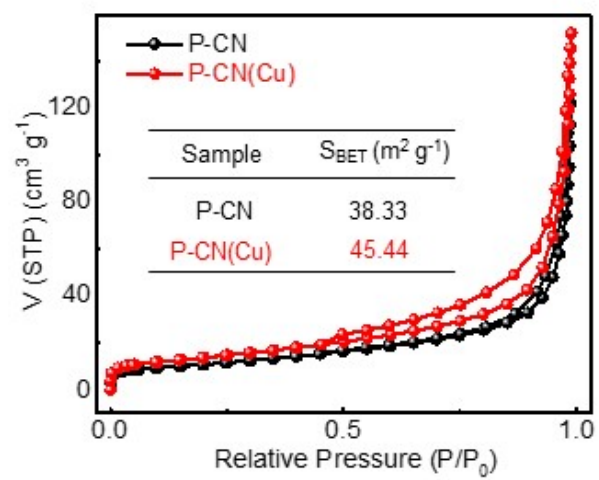


**Fig. S4.**  $\text{N}_2$  adsorption-desorption isotherms of P-CN(Cu) and P-CN.

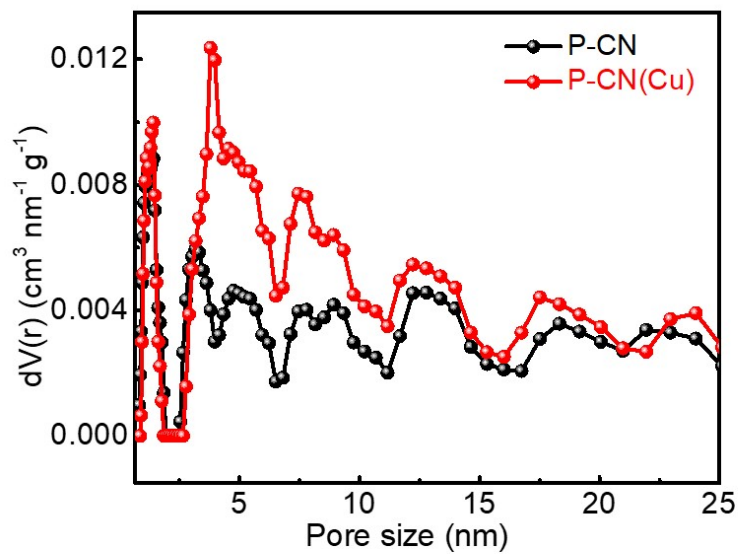


**Fig. S5.** Pore size distribution curves of P-CN(Cu) and P-CN.

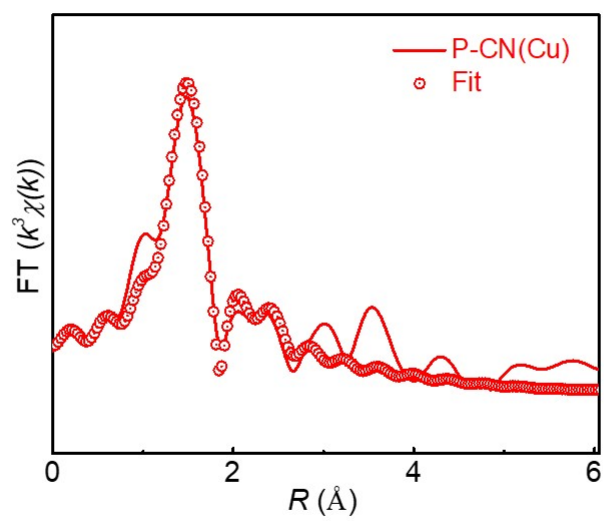


**Fig. S6.** EXAFS fitting curve of P-CN(Cu).

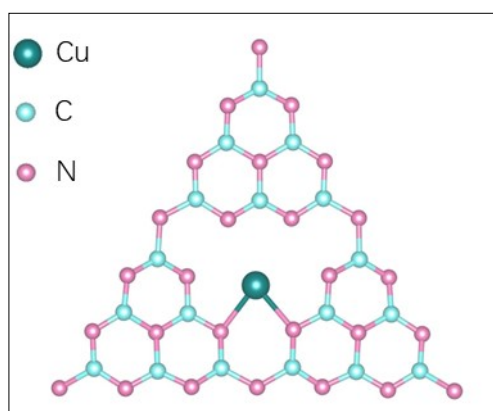


**Fig. S7.** Coordination configuration of Cu in P-CN(Cu).

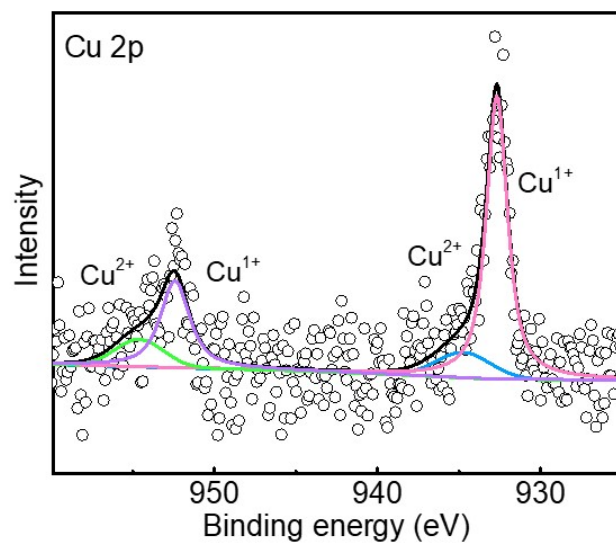


**Fig. S8.** High-resolution XPS spectrum of Cu 2p of P-CN(Cu).

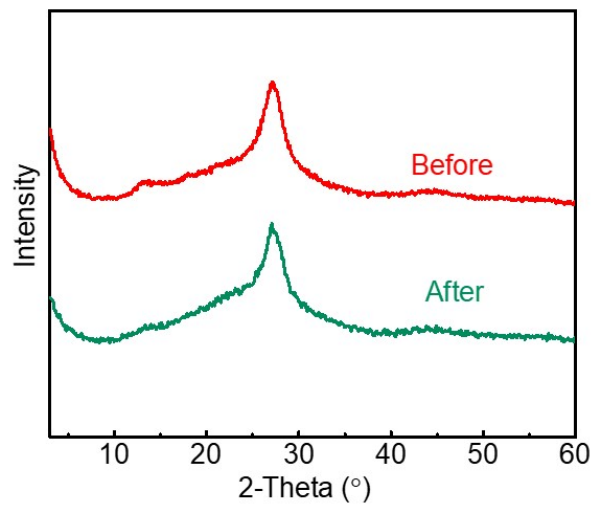


**Fig. S9.** XRD patterns of the P-CN(Cu) before and after photocatalytic reaction.

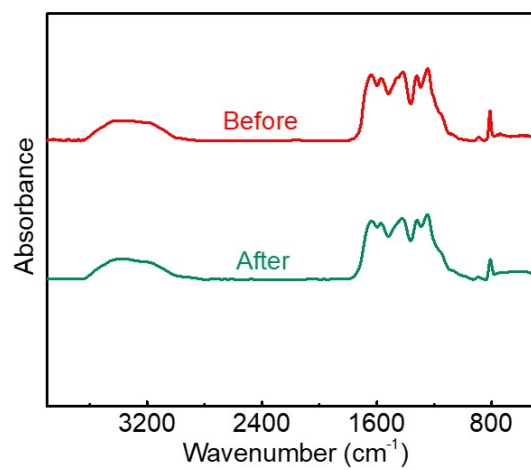


**Fig. S10.** FT-IR spectra of the P-CN(Cu) before and after photocatalytic reaction.

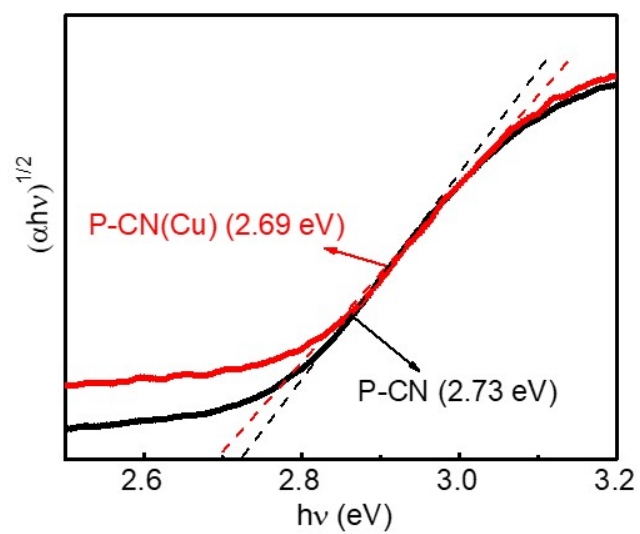


**Fig. S11.** Band gap energies of P-CN(Cu) and P-CN.

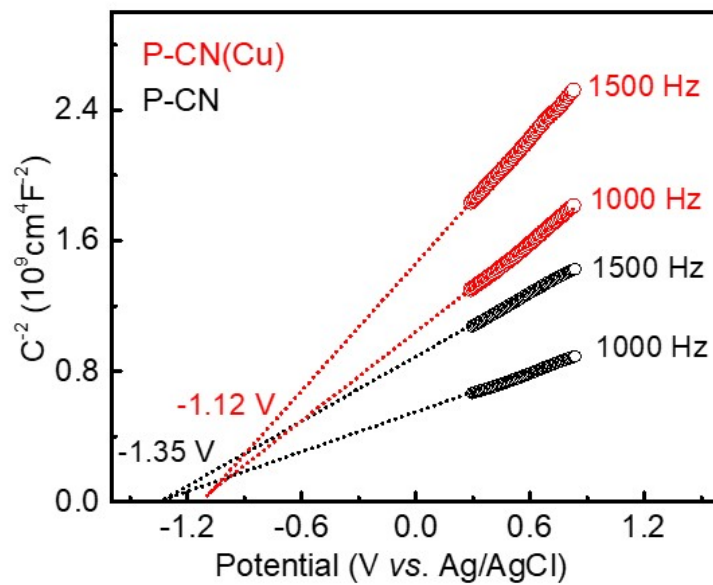


**Fig. S12.** Mott-Schottky plots of P-CN(Cu) and P-CN.

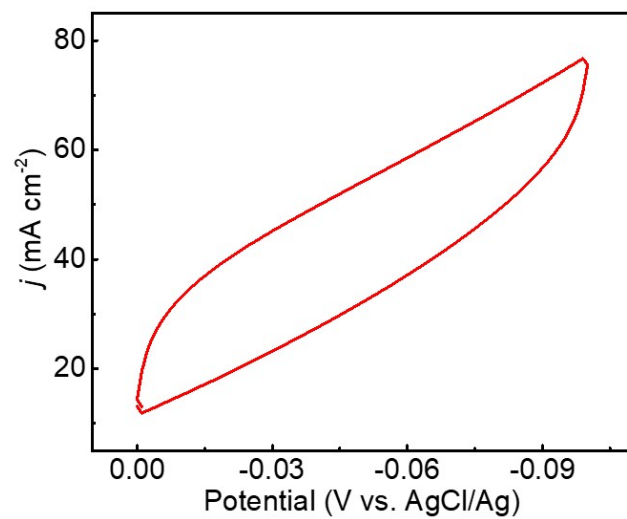


**Fig. S13.** Cyclic voltammetry curve of P-CN(Cu).

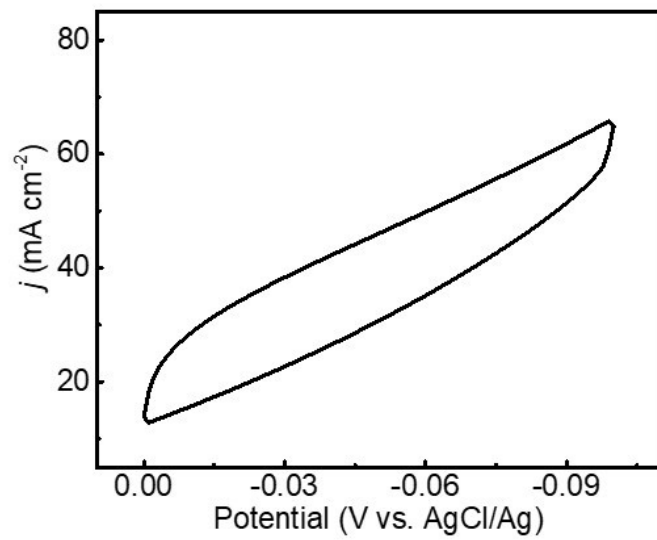


**Fig. S14.** Cyclic voltammetry curve of P-CN.

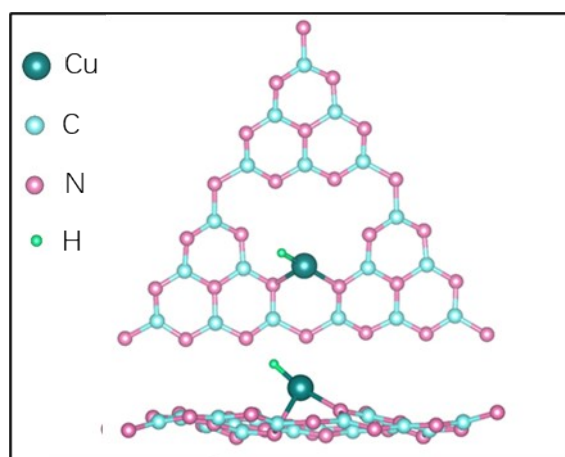


**Fig. S15.** Structure model of H<sup>+</sup> adsorbed on P-CN(Cu).

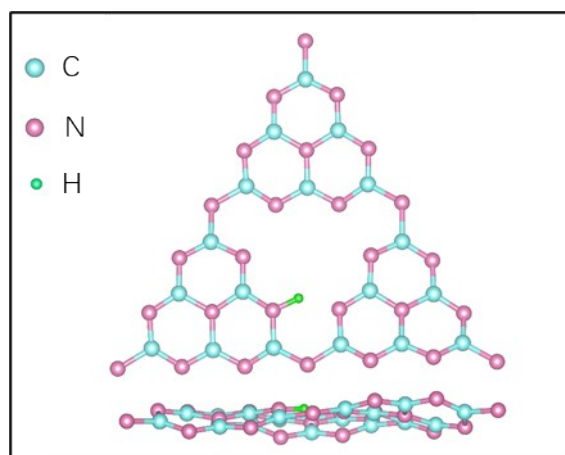


**Fig. S16.** Structure model of H<sup>+</sup> adsorbed on P-CN.

**Table S1.** EXAFS fitting of P-CN(Cu).

Sample	Shell	$N^a$	$R$ (Å) $^b$	$\sigma^2$ (Å <sup>-2</sup> ·10 <sup>-3</sup> ) $^c$	$\Delta E_0$ (eV) $^d$
P-CN(Cu)	Cu-N	2.4 (~2)	1.95	0.002	6.8

$N^a$ : average coordination numbers.  $R^b$ : average interatomic distance.  $\sigma^2$  (Å<sup>-2</sup>·10<sup>-3</sup>)  $^c$ : Debye-Waller factor.  $\Delta E_0$  (eV)  $^d$ : edge-energy shift.

**Table S2.** High-resolution XPS spectra fitting data of N 1s for P-CN(Cu) and P-CN.

Sample N 1s	P-CN(Cu)		
	Position (eV)	FWHM (eV)	Area
N-Hx	400.9	1.653	17821.21
N-(C) <sub>3</sub> (N <sub>3C</sub> )	399.2	1.630	35161.95
C=N-C(N <sub>2C</sub> )	398.7	1.158	47249.92

The peak area ratio of N<sub>2C</sub>/N<sub>3C</sub> for P-CN(Cu) is 1.34.

Sample N 1s	P-CN		
	Position (eV)	FWHM (eV)	Area
N-Hx	401.1	1.092	12886.17
N-(C) <sub>3</sub> (N <sub>3C</sub> )	400.0	1.372	27353.88
C=N-C(N <sub>2C</sub> )	398.6	1.200	125416.70

The peak area ratio of N<sub>2C</sub>/N<sub>3C</sub> for P-CN is 4.58.